4-20-2006

Buoyancy generated turbulence in stably stratified flow with shear

Jin Hwan Hwang
Korea Environment Institute

Hidekatsu Yamazaki
Tokyo University of Marine Science and Technology

Chris R. Rehmann
Iowa State University, rehmann@iastate.edu

Buoyancy generated turbulence in stably stratified flow with shear

Jin H. Hwang, Hidekatsu Yamazaki, and Chris R. Rehmann

Citation: Physics of Fluids (1994-present) **18**, 045104 (2006); doi: 10.1063/1.2193472
View online: http://dx.doi.org/10.1063/1.2193472
View Table of Contents: http://scitation.aip.org/content/aip/journal/pof2/18/4?ver=pdfcov
Published by the AIP Publishing

Buoyancy generated turbulence in stably stratified flow with shear

Jin H. Hwang
Korea Environment Institute, 613-2, Bulkwang-Dong, Eunpyung-Gu, Seoul 122-040, Republic of Korea

Hidekatsu Yamazaki
Department of Ocean Sciences, Tokyo University of Marine Science and Technology, 4-5-7 Konan, Minato-ku, Tokyo 108-8477, Japan

Chris R. Rehmann
Department of Civil, Construction, and Environmental Engineering, Iowa State University, Ames, Iowa 50011

(Received 7 July 2005; accepted 10 January 2006; published online 20 April 2006)

The energy evolution in buoyancy-generated turbulence subjected to shear depends on the gradient Richardson number Ri and the stratification number St, which is a ratio of the time scale of the initial buoyancy fluctuations to the time scale of the mean stratification. During an initial period, the flow state evolves as in the unsheared case. After this period, shear generates fluctuating velocity components for St=0.25, but it depletes the fluctuating vertical velocity component and temperature variance faster than in the unsheared case for St=4. Weak shear causes the kinetic and total energy to decrease faster than in the unsheared case, whereas strong shear adds more energy in comparison with the unsheared case. Energy increased with time in only one case considered (St=0.1 and Ri =0.04). When St>1, the nonlinearity of the flow does not become significant even when Ri is small. Thus, results from rapid distortion theory and direct numerical simulation compare well. In particular, the theory reproduces trends in the energy evolution for St>1. © *2006 American Institute of Physics*. [DOI: 10.1063/1.2193472]

I. INTRODUCTION

Even after turbulence decays in a stably stratified flow, fluctuations of active scalars, such as temperature or salinity, can remain. Gerz *et al.*[1] and Ramsden and Holloway[2] found that more potential energy than kinetic energy exists near dissipation scales because the rates of transfer of kinetic and potential energy differ. Flows in which scalar fluctuations indicate a previous turbulent event that has decayed have been called "fossil turbulence" (e.g., Woods *et al.*,[3] Nasmyth,[4] and Gibson *et al.*[5]). As the remnant fluctuations of potential energy adjust under the restoring force of gravity, they can generate internal waves and turbulence. If turbulence develops again from the remnant state, mixing and transport of scalars can occur.[6] Previous work on remnant potential energy focused on the existence of potential energy fluctuations after kinetic energy decayed. We investigate whether remnant potential energy can interact with the mean velocity field to regenerate the kinetic energy of the turbulence.

Effects of mean shear have been studied for stratified turbulence activated by initial velocity fluctuations (e.g., Rohr *et al.*,[7] Holt *et al.*,[8] and Jacobitz *et al.*[9]). A key parameter for this flow is the gradient Richardson number

$$\mathrm{Ri} = \frac{N^2}{(\partial U/\partial z)^2} = \frac{N^2}{S^2}, \tag{1}$$

where S is the shear rate, the buoyancy frequency is

$$N = \left(\alpha g \frac{d\Theta}{dz}\right)^{1/2}, \tag{2}$$

α is the thermal expansion coefficient, Θ is temperature, and g is the acceleration of gravity; when the stratification is stable, as in the flow studied here, the temperature gradient is positive. If the Richardson number is smaller than a "stationary Richardson number," the turbulent kinetic energy increases with time.[7] Several researchers have investigated the dependence of the flow evolution and, in particular, the stationary Richardson number Ri_s on other parameters: At low Reynolds number, Ri_s increases with increasing Reynolds number[8] but also depends on the shear number,[9] which is the ratio of a time scale of the large eddies and the time scale of the shear. At a higher Reynolds number, the shear number approaches a constant, and Ri_s depends only on the Reynolds number.[10] Shih *et al.*[10] also recommended using a Froude number based on turbulence scales for studying the physics of a flow.

The evolution of turbulence activated by initial potential energy fluctuations was investigated by Gerz and Yamazaki.[11,12] For a flow without shear, Gerz and Yamazaki[11] (abbreviated GY), on which the present work is based, showed the importance of the stratification number

$$\mathrm{St} = \frac{l_T}{T_0'}\frac{d\Theta}{dz}, \tag{3}$$

where l_T is the integral length scale of the initial temperature spectrum and T_0' is the initial root mean square (rms) temperature fluctuation. The stratification number St measures

the strength of initial gravitational collapse by comparing the length scale of the initial temperature field to the Ellison scale $T_0'/(d\Theta/dz)$. In supercritical flow ($\mathrm{St}<1$), the initial potential energy fluctuations are large enough for nonlinear motions typical of turbulence to develop, and in subcritical flow ($\mathrm{St}>1$), the flow has features more typical of internal waves. In a preliminary study, Gerz and Yamazaki[12] added mean shear to the flows simulated by GY: Over the range of St considered, total energy always decreased after half a buoyancy period.

The present work investigates the evolution of buoyancy-generated turbulence subjected to uniform mean shear. We focus on whether the shear can reenergize the flow, and we determine flow characteristics for various stratification and Richardson numbers. In particular, the growth of total energy in sheared cases is compared with that in the unsheared case. We also study the nonlinearity of the flow by comparing the results from direct numerical simulation (DNS) and rapid distortion theory (RDT). Since RDT works well when nonlinearity is weak, RDT can help identify the role of linear processes relative to nonlinear processes.

TABLE I. Parameters of the direct numerical simulations.

Case	St	Ri	Re	No. of grid points
AS1	0.1	0.04	11.6	64^3
AS2	0.1	0.25	11.6	64^3
BS1	0.25	0.16	57.4	128^3
BS2	0.25	0.25	57.4	64^3
BS3	0.25	0.5	57.4	64^3
BS4	0.25	1	57.4	64^3
BS5	0.25	∞	57.4	64^3
CS1	0.5	0.16	57.4	64^3
CS2	0.5	0.25	57.4	64^3
CS3	0.5	0.5	57.4	64^3
CS4	0.5	1	57.4	64^3
DS1	0.75	0.16	57.4	64^3
DS2	0.75	0.25	57.4	64^3
DS3	0.75	1	57.4	64^3
FS1	4	0.01	57.4	64^3
FS2	4	0.08	57.4	64^3
FS3	4	0.16	57.4	64^3
FS4	4	1	57.4	64^3
FS5	4	10	57.4	64^3
FS6	4	∞	57.4	64^3

II. METHODS

A. Direct numerical simulation

The simulations are similar to those in Gerz and Yamazaki.[11,12] Perturbation velocities $(u_1,u_2,u_3)=(u,v,w)$ and perturbation temperature T are computed in a cubic domain. Periodic boundary conditions are used because the turbulence is homogeneous and the mean horizontal background velocity $U(z)$ and temperature $\Theta(z)$ are linear functions of the vertical coordinate z. Thus, the vertical gradients of mean velocity and temperature are constant.

The Navier-Stokes equations and the temperature equation with the Boussinesq approximation are solved in dimensionless form. Density is scaled by a reference density ρ^*, and time is scaled by the buoyancy time scale $2\pi/N$. The temperature fluctuation is made dimensionless with the initial rms temperature $(\overline{T_0^2})^{1/2}=T_0'$, and lengths are scaled by the initial integral length scale of the temperature spectrum $S(k)$:

$$l_T=\frac{1}{2}\pi\int\frac{1}{k}S(k)dk, \tag{4}$$

where the magnitude of the wave number is $k=(k_1^2+k_2^2+k_3^2)^{1/2}$ and $S(k)$ is the initial spectrum function of the temperature fluctuations. As a result of these scaling choices, velocities are scaled by Nl_T. The nondimensional governing equations become

$$\frac{\partial u_i}{\partial t}+\frac{\partial}{\partial x_j}(u_ju_i)+\mathrm{Ri}^{-1/2}x_3\frac{\partial u_i}{\partial x_1}+\mathrm{Ri}^{-1/2}u_3\delta_{i1}=\mathrm{Re}^{-1}\frac{\partial^2 u_i}{\partial x_j^2}-\frac{\partial p}{\partial x_i}+\mathrm{St}^{-1}T\delta_{i3}, \tag{5a}$$

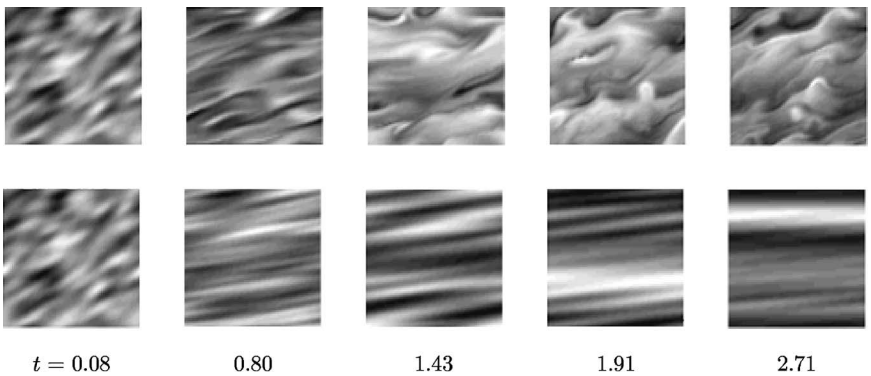

FIG. 1. Evolution of the temperature field in the x-z plane. Darker shades indicate positive temperature fluctuations and lighter shades indicate negative temperature fluctuations. The case in the top row has St=0.1 and Ri=0.04 and the case in the bottom row has St=4 and Ri=1.

$$\frac{\partial T}{\partial t} + \frac{\partial}{\partial x_j}(u_j T) + \mathrm{Ri}^{-1/2} x_3 \frac{\partial T}{\partial x_1} + \mathrm{St} u_3 = \mathrm{Re}^{-1}\mathrm{Pr}^{-1}\frac{\partial^2 T}{\partial x_j^2}, \tag{5b}$$

$$\frac{\partial u_i}{\partial x_i} = 0. \tag{5c}$$

The flow is governed by several nondimensional parameters. For unsheared, buoyancy-generated turbulence, GY identified the Reynolds number $\mathrm{Re}=Nl_T^2/\nu$, the Prandtl number $\mathrm{Pr}=\nu/D$, and the stratification number St, and they classified cases with $\mathrm{St}>1$ as subcritical and cases with $\mathrm{St}<1$ as supercritical. For sheared, buoyancy-generated turbulence, the gradient Richardson number Ri is also important. Because the vertical gradients of mean velocity and temperature are constant, the Richardson, Reynolds, and stratification numbers are also constant in each simulation. We kept the temperature gradient constant throughout the simulations and varied l_T and T_0' to obtain desired values of St and Re. The shear rate S was varied to set values of Ri.

The initial conditions for buoyancy-generated turbulence consist of zero initial velocity fluctuations and temperature fluctuations that have random phase and a spectral shape given by

$$S(k) = \frac{16}{2\pi}\left(\frac{2}{\pi}\right)^{1/2}\frac{k^4}{k_p^5}\exp[-2(k/k_p)^2], \tag{6}$$

where the magnitude of the nondimensional peak integer wave number k_p is $(8\pi)^{1/2}$. We set $\mathrm{Pr}=1$ for all runs and $\mathrm{Re}=57.4$ for all runs except two cases with $\mathrm{St}=0.1$; in those cases, smaller Re was used so that the flow could be properly resolved. Aside from the case with $\mathrm{St}=0.1$, we studied the effect of shear on the flows that GY investigated. Values of the stratification number include subcritical ($\mathrm{St}=0.25$) and supercritical ($\mathrm{St}=4$) cases, and the Richardson number is varied over a range that allows for growth and decay of turbulence (Table I). Dissipation spectra were examined to ensure that the simulations resolve the flow adequately. All flows are simulated in a computational domain of size 4π for three buoyancy periods using a time step of $2\Delta x/3$, where Δx is the grid spacing on a side. Details of the numerical method can be found in Gerz *et al.*[1]

B. Rapid distortion theory

RDT applies when the time scale of the mean flow is small compared to the time scale of the turbulence. Hanazaki and Hunt[13] compared the buoyancy time scale N^{-1} to an eddy time scale λ/u_λ and obtained a criterion for the validity of RDT in terms of the Froude number $\mathrm{Fr}=u_\lambda/\lambda N$. In particular, RDT applies to scales λ and larger when $\mathrm{Fr}<1$. For buoyancy-generated turbulence, a similar criterion using the stratification number can be derived with a time scale based on l_T. Because $(l_T/b_0')^{1/2}$ is a time scale of eddies in the initial turbulence field (where $b_0'=g\alpha T_0'$) and N^{-1} is the buoyancy time scale, the stratification number can be written as a (squared) ratio of turbulence and mean time scales:

$$\mathrm{St} = \frac{l_T}{T_0'}\frac{d\Theta}{dz} = \frac{l_T/b_0'}{1/N^2}. \tag{7}$$

Therefore, RDT should apply to buoyancy-generated turbulence when $\mathrm{St}>1$.

After nonlinear terms in the governing equations are neglected, the equations are expressed in terms of coordinates that follow the mean flow:

$$\xi_1 = x_1 - tSx_3, \quad \xi_2 = x_2, \quad \xi_3 = x_3. \tag{8}$$

This transformation facilitates solution by Fourier methods, in which the velocities are expressed as

$$u_j(\xi,t) = \sum_{\underline{k}} \hat{u}_j(\underline{k},t)e^{-ik_j\xi_j}, \tag{9}$$

where k_j is the wave number in the j direction and the hats denote Fourier amplitudes. After pressure is eliminated with the continuity equation, Eqs. (5a) and (5b) become

$$\frac{d\hat{u}_1}{dt} = \mathrm{Ri}^{-1/2}\left(\frac{2k_1^2}{K^2} - 1\right)\hat{u}_3 + \mathrm{St}^{-1}\frac{k_1K_3}{K^2}\hat{T} - \mathrm{Re}^{-1}K^2\hat{u}_1, \tag{10a}$$

$$\frac{d\hat{u}_2}{dt} = 2\mathrm{Ri}^{-1/2}\frac{k_1k_2}{K^2}\hat{u}_3 + \mathrm{St}^{-1}\frac{k_2K_3}{K^2}\hat{T} - \mathrm{Re}^{-1}K^2\hat{u}_2, \tag{10b}$$

$$\frac{d\hat{u}_3}{dt} = 2\mathrm{Ri}^{-1/2}\frac{k_1K_3}{K^2}\hat{u}_3 + \mathrm{St}^{-1}\left[\frac{K_3^2}{K^2} - 1\right]\hat{T} - \mathrm{Re}^{-1}K^2\hat{u}_3, \tag{10c}$$

$$\frac{d\hat{T}}{dt} = \mathrm{St}\hat{u}_3 - \mathrm{Re}^{-1}\mathrm{Pr}^{-1}K^2\hat{T}, \tag{10d}$$

where

$$K_3 = k_3 - k_1\mathrm{Ri}^{-1/2}t,$$
$$K^2 = k^2 - 2k_1k_3\mathrm{Ri}^{-1/2}t + k_1^2\mathrm{Ri}^{-1}t^2, \quad k^2 = k_mk_m. \tag{11}$$

Spectra are computed with a discrete Fourier transform of the two-point correlations; for example,

$$E_{T3}(\underline{k},t) = \lim_{V\to\infty}\frac{V}{(2\pi)^3}\langle\hat{T}\hat{u}_3^+\rangle, \tag{12}$$

where the plus sign superscript denotes complex conjugate and the angle brackets denote ensemble average. Equations for the spectra can be derived using (10) and (12); for example, the equation for the co-spectrum of vertical velocity and temperature is

$$\frac{dE_{T3}}{dt} = 2\mathrm{Ri}^{-1/2}\frac{k_1K_3}{K^2}E_{T3} + \mathrm{St}^{-1}\left(\frac{K_3^2}{K^2} - 1\right)E_{TT} + \mathrm{St}\,E_{33} - \mathrm{Re}^{-1}(1+\mathrm{Pr}^{-1})K^2E_{T3}. \tag{13}$$

Equations for spectra are solved numerically, and turbulence statistics are then obtained by integrating the spectra over wave number space.

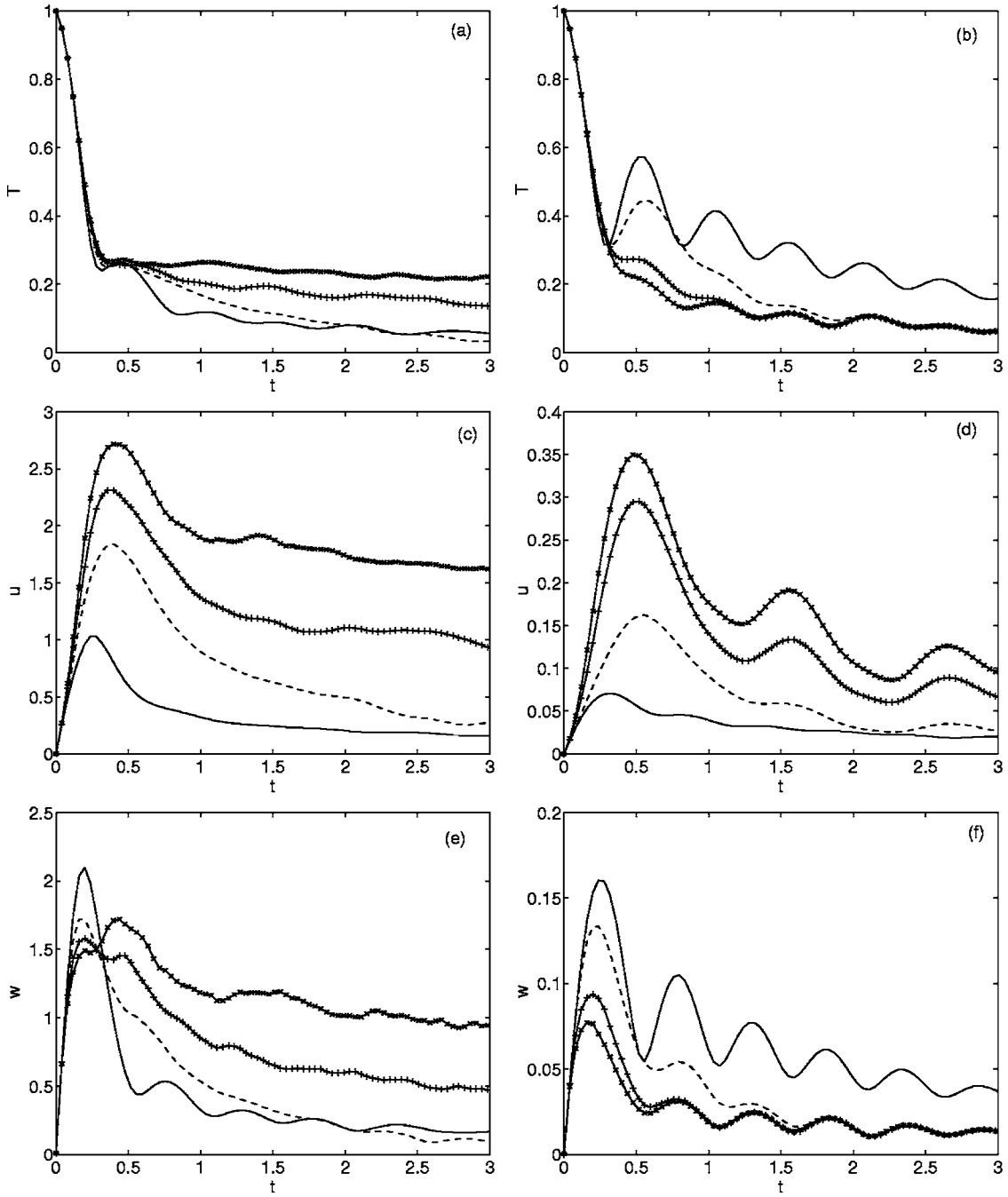

FIG. 2. Root mean square temperature and velocities. The stratification number is 0.25 in (a), (c), and (e): unsheared flow (Ri$\rightarrow\infty$) (—); Ri=1 (---); 0.25 (-+-); and 0.16 (-×-). The stratification number is 4 in (b), (d), and (f): unsheared flow (Ri$\rightarrow\infty$) (—); Ri=1 (---); 0.16 (+); and 0.08 (×).

III. RESULTS

The flow features observed in the DNS are presented in this section. The extent to which RDT reproduces the flow features is discussed in Sec. IV.

A. Temperature fields

The evolution of the temperature fluctuations depends on the values of St and Ri (Fig. 1). At $t=0.08$, the temperature fields from the two cases resemble each other; in both cases, striations in the temperature field are inclined at approximately 45° to the flow direction. For $t>0.08$ the flow with St=0.25 continues to have vertical and horizontal structures, whereas the flow with St=4 shows only horizontal striations like those seen in the final period of wake decay.[14] Such patterns of evolution are observed in the subcritical cases for all Ri and the weakly sheared supercritical cases.

B. RMS quantities

The evolution of the rms quantities can be divided into two phases (Fig. 2). For $t<0.25$, the behavior is similar to that in the unsheared case because the buoyancy of the initial temperature field mainly drives the flow. During this phase,

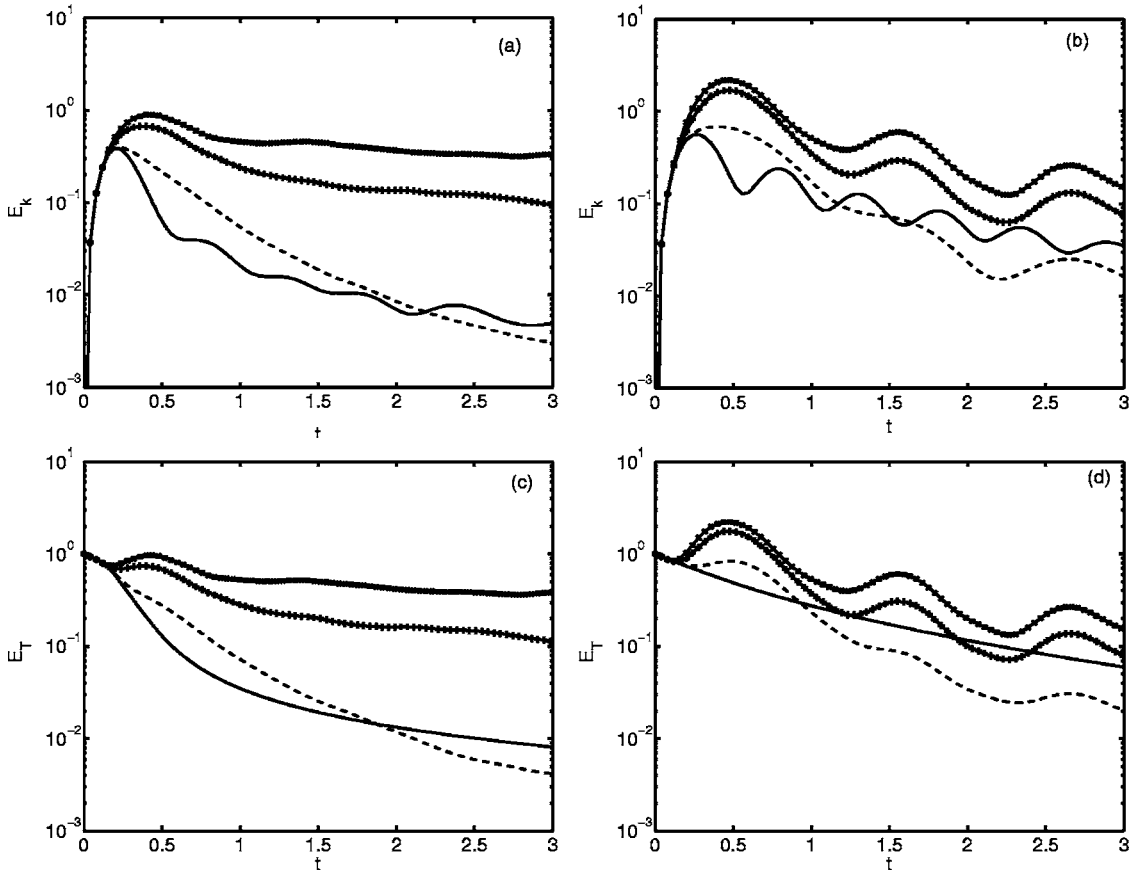

FIG. 3. Evolution of kinetic energy [(a) and (b)] and total energy [(c) and (d)]. The stratification number is 0.25 in (a) and (c), and 4 in (b) and (d). Lines are as in Fig. 2.

the normalized rms temperature does not depend on St and Ri; in all cases the time series are nearly identical [Figs. 2(a) and 2(b)].

For $t>0.25$, the evolution of the rms quantities depends strongly on St and Ri. The rms temperature continues to decrease in time in all runs with St=0.25. The lowest Ri case shows the least decline, and the cases with no shear and Ri =1 show almost identical reduction. The rms temperature for St=4 oscillates for all values of Ri. When no shear is present, the period is approximately half a buoyancy period, as in GY. Somewhat surprising is that the amplitude of the rms temperature fluctuation is reduced when the background shear is increased. The rms streamwise velocity increases with decreasing Ri for flows with both St=0.25 and St=4 [Figs. 2(c) and 2(d)]. Like the rms temperature, the rms streamwise velocity also oscillates for St=4, but the period is approximately twice that observed for the rms temperature.

The evolution of the rms vertical velocity resembles the evolution of the rms temperature in many ways [Figs. 2(e) and 2(f)]. Because vertical velocity fluctuations are created at the expense of the rms temperature, the oscillations for St =4 appear with the same period as those in T, but w is out of phase with T. Like the amplitude of oscillations of rms temperature, the amplitude of oscillations in rms vertical velocity decreases as Ri decreases when St=4 [Fig. 2(f)]. The rms temperature and vertical velocity depend similarly on the Richardson number: Both increase with increasing shear (or decreasing Ri) for St=0.25, and both decrease with increasing shear when St=4. Also, for St=4, both the rms temperature and vertical velocity reach values independent of Ri after two buoyancy periods; in all subcritical cases with finite shear, the vertical velocity and temperature fluctuations converge to a similar value.

C. Energy

Like the rms quantities, the energy also shows two phases of evolution (Fig. 3). In the initial phase ($t<0.25$) when the initial density fluctuations are adjusting, the turbulent kinetic energy increases at the expense of the turbulent potential energy, which is proportional to the square of the rms temperature. During this phase, the kinetic energy in all of the sheared flows is larger than that of the unsheared flow. However, the kinetic energy and the total energy for all cases decrease after $t>0.5$, for the parameter range in Fig. 3. In fact, for flows with both St=0.25 and 4, the kinetic and the total energy fall below those of the unsheared flow when Ri=1.

Because nonlinearities are strongest in supercritical flows (GY) and energy increases in time in flows with low Richardson number, active turbulence for sheared buoyancy-generated turbulence should occur when St<1 and the Richardson number is small. However, when St=0.25, the kinetic energy decreases with time [Fig. 3(a)] even for Ri

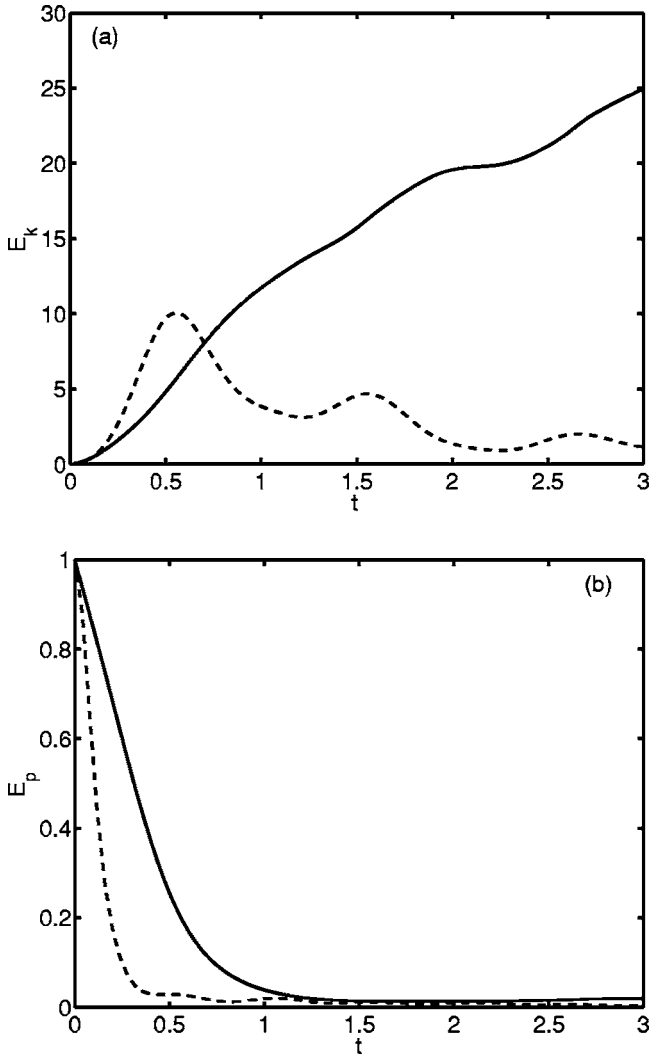

FIG. 4. Evolution of (a) kinetic energy and (b) potential energy: St=0.1, Ri=0.04 (—) and St=4, Ri=0.01 (---).

=0.16, which is smaller than the value of 0.25 approached in turbulence with high Reynolds number.[8] In sheared, stratified turbulence with initial velocity fluctuations, the stationary Richardson number decreases with decreasing Reynolds number based on final values of integral scales. In buoyancy-generated turbulence, decreasing St and Ri further yields growing turbulence: When St=0.1 and Ri=0.04 the kinetic energy increases with time [Fig. 4(a)], and the potential energy decreases until it reaches a plateau after approximately one buoyancy period [Fig. 4(b)]. In a subcritical flow, both the kinetic energy and potential energy decrease even when Ri=0.01; whereas the kinetic energy has a larger peak value than in other subcritical cases, it eventually decreases with time. Shear never generated sustained turbulence in subcritical cases.

Energy spectra illustrate the differences between weakly and strongly sheared flows. Weak shear apparently drains the energy faster than in the unsheared case. Energy spectra for a supercritical flow show that energy in the low wave numbers decreases [Fig. 5(a)] and the peak of the dissipation spectrum shifts from high to low wave number [Fig. 5(b)]; thus, the energy cascade occurs as observed in decaying stratified turbulence. In the strongly sheared, supercritical case, low wave numbers gain energy [Fig. 5(c)], and the DNS resolves the relevant small scales, as the dissipation spectra show [Fig. 5(d)].

D. Momentum and heat flux

In supercritical flow, the momentum flux $\overline{uw}$ is down-gradient (i.e., negative) and constant with time for all cases except when Ri=1 [Fig. 6(a)]. On the other hand, the momentum flux in subcritical flow oscillates between down-gradient and up-gradient with a frequency close to the buoyancy frequency. The streamwise heat flux $\overline{uT}$ in supercritical flow either remains nearly constant or increases slightly for $t>0.5$ [Fig. 6(c)]; this feature appears in the weakly stratified, unsheared wind tunnel experiments of Lienhard and Van Atta.[15] The flux $\overline{uT}$ is approximately 0.5 at large times in both subcritical and supercritical flows, though it varies more in the subcritical case [Fig. 6(d)].

The behavior of the vertical heat flux depends strongly on the stratification number. In both subcritical and supercritical cases, the vertical heat flux is initially up-gradient ($\overline{wT}>0$) because the initial temperature fluctuations adjust [Figs. 6(e) and 6(f)]. The vertical heat flux approaches a constant in the supercritical flows with the strongest shear, but when Ri>0.25, oscillations appear and the flux becomes up-gradient [Fig. 6(e)]. The subcritical flow has large-amplitude oscillations that depend very little on the Richardson number. In unsheared buoyancy-generated turbulence, the vertical heat flux changed from up-gradient to down-gradient when the kinetic energy reached a maximum. With shear, however, the peak in kinetic energy occurs after the heat flux changes sign, and the delay is larger for smaller Richardson number, or stronger shear.

IV. DISCUSSION

A. Mixing states

Subcritical flows and supercritical flows with weak shear cannot sustain down-gradient heat flux. In fact, in their preliminary study of this problem, Gerz and Yamazaki[12] assumed that the oscillating fluxes resulted from shear forcing internal wave modes in near-laminar flow. For subcritical flows, the horizontal striations at large times (Fig. 1), the phase difference between w and T, and the collapse of w and T in the weakly sheared cases for $t>2$ support this assumption. Further insight into the state of the flow and its ability to sustain active mixing can be obtained by examining the normalized dissipation, $\varepsilon/\nu N^2$. The behavior of $\varepsilon/\nu N^2$ differs considerably between cases with St=0.25 and St=4 (Fig. 7). For St=0.25, even though $\varepsilon/\nu N^2$ decreases rapidly below 10 in the cases with no shear and Ri=1, initially $\varepsilon/\nu N^2$ is large in all cases. For St=4, $\varepsilon/\nu N^2$ remains below 10 throughout the evolution.

The normalized dissipation $\varepsilon/\nu N^2$ has been interpreted as a measure of the range of length scales available for active mixing. This parameter is equivalent to $(L_O/\eta)^{4/3}$, where $L_O=(\varepsilon/N^3)^{1/2}$ is the Ozmidov scale, a measure of the smallest scale that experiences significant effects of gravitational

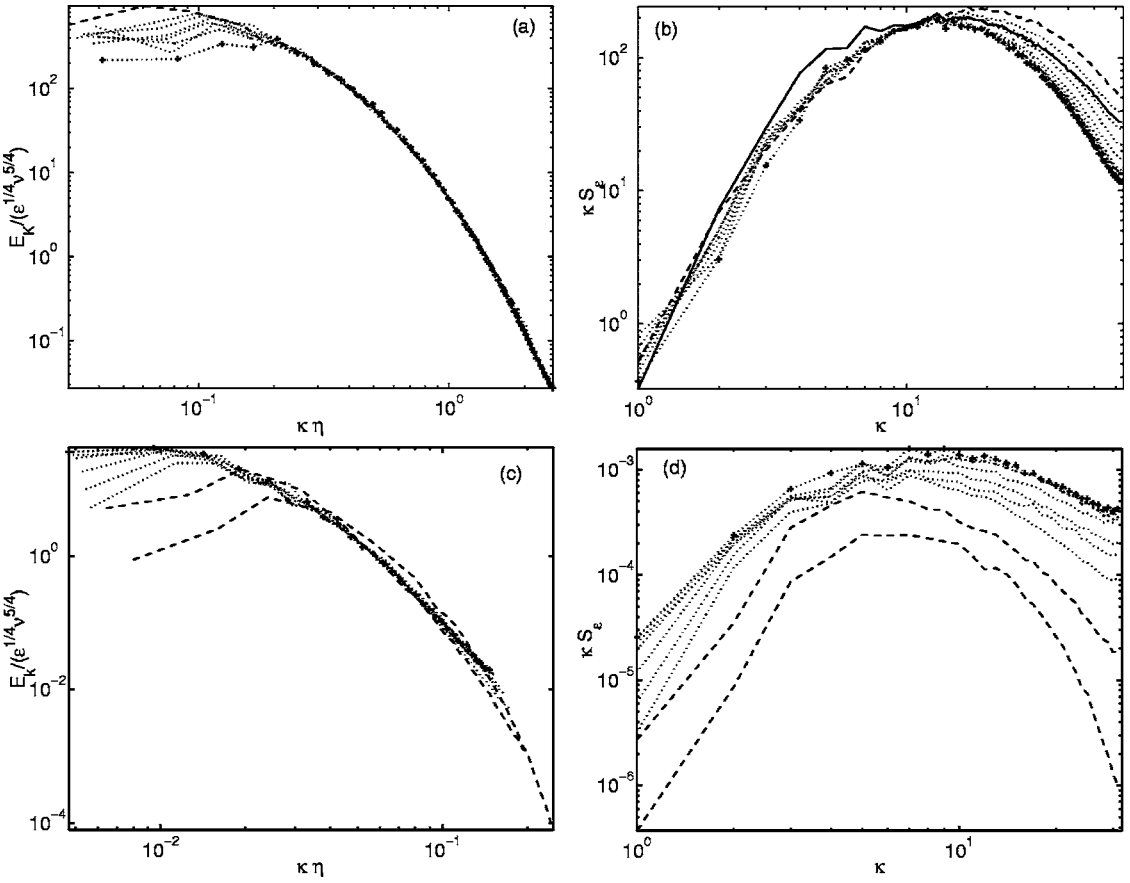

FIG. 5. Kinetic energy spectra E_K and dissipation spectra S_ε. The stratification number is 0.25 and the Richardson number is 0.16 in (a) and (b) and the stratification number is 0.1 and the Richardson number is 0.04 in (c) and (d): $t<0.25$ (---); $0.25<t<3$ (—); and $t=3$ (-+-).

adjustment and $\eta=(\nu^3/\varepsilon)^{1/4}$ is the Kolmogorov scale, the smallest scale in the velocity field. Because motions larger than the Ozmidov scale cannot overturn, the range of length scales that can overturn is small when $\varepsilon/\nu N^2$ is small. For example, Smyth and Moum[16] found that when $\varepsilon/\nu N^2>20$ a three-dimensional turbulent flow can occur, whereas when $\varepsilon/\nu N^2<20$, the flow consists mainly of internal waves. Yamazaki[17] also suggested $\varepsilon/\nu N^2=16$ to differentiate a state of active mixing from one without active mixing. These criteria suggest that when $\mathrm{St}<1$, active mixing occurs at least initially, whereas when $\mathrm{St}>1$, no significant mixing should occur for all values of Ri we investigated.

Recently, Shih *et al.*[18] identified three regimes of energetics for a sheared, stratified flow with initial velocity fluctuations: a diffusive regime for $\varepsilon/\nu N^2<7$, in which molecular diffusion controls vertical fluxes; an intermediate regime for $7<\varepsilon/\nu N^2<100$, in which the eddy diffusivity follows the relationship of Osborn;[19] and an energetic regime for $\varepsilon/\nu N^2>100$, in which the total diffusivities are greater than 10 times the molecular diffusivity. Applied to our flow, these observations suggest that the subcritical cases and the weakly sheared supercritical cases are in the diffusive regime, and both our flow and that of Shih *et al.*[18] showed oscillating vertical momentum and scalar fluxes when $\varepsilon/\nu N^2$ is small. These results support the suggestion[12] that in these cases the flow is close to laminar.

B. Energy evolution

Strong shear adds more energy in comparison with the unsheared case for both $\mathrm{St}=0.25$ and 4. The total energy in the two cases with the lowest Richardson number for $\mathrm{St}=0.25$ and the case with the lowest Richardson number for $\mathrm{St}=4$ always exceeds that from the unsheared flow (Fig. 3). However, strong shear energizes the flow in different ways depending on the stratification number, or the magnitude of the initial gravitational collapse. When the flow is supercritical ($\mathrm{St}<1$), strong shear energizes all velocity components [Figs. 2(c) and 2(e)], and a three-dimensional turbulent flow is generated. However, when the flow is subcritical ($\mathrm{St}>1$), shear energizes only the velocity in the direction of flow, and the other velocity fields diminish according to the intensity of shear [Figs. 2(d) and 2(f)]. Shear neither generates nonlinear turbulence nor contributes significantly to mixing. As we discuss in Sec. IV C, when the flow is subcritical, nonlinearity is less important.

In contrast, weak shear plays a role in decreasing the energy. When $\mathrm{Ri}=1$ for both $\mathrm{St}=0.25$ and $\mathrm{St}=4$, initially the sheared flows have more energy than the unsheared flow, but as time passes, the total and the kinetic energies become less than that of the unsheared flow (Fig. 3). Gerz and Schumann[6] observed similar behavior in stratified turbulence with initial velocity fluctuations; flows with $\mathrm{Ri}=0.66$ and 1.32 had less

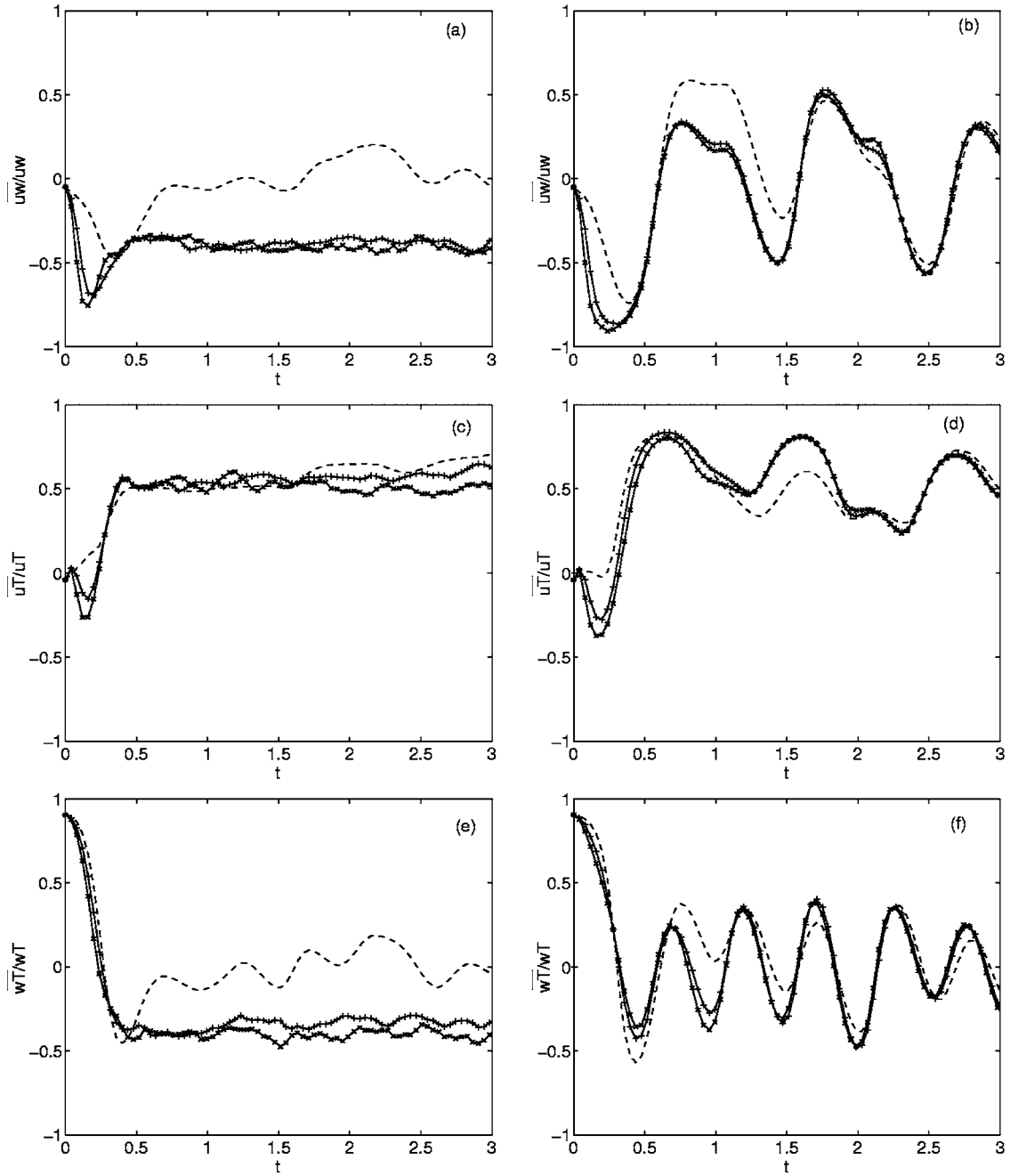

FIG. 6. Correlation coefficients: (a) and (b) present the Reynolds stress, or the vertical momentum flux; (c) and (d) show the streamwise heat flux; and (e) and (f) show the vertical heat flux. The stratification number is 0.25 in (a), (c), and (e): Ri=1 (---); 0.25 (-+-); and 0.16 (-×-). The stratification number is 4 in (b), (d), and (f): Ri=1 (---); 0.16 (-+-); and 0.08 (-×-).

total energy than their unsheared counterparts by the end of the simulation. They suggested that this unexpected behavior could be due to two mechanisms: (1) wave breaking from low Richardson number at small scales and (2) negative production of turbulent kinetic energy caused by up-gradient momentum flux. Gerz and Schumann[6] presented the larger dissipation in sheared cases as evidence for the first mechanism and the persistent up-gradient values of $\overline{uw}$ they observed for Ri=0.66 and 1.32 as support for the latter mechanism.

Of the two mechanisms, a variant of the second is more likely to explain the faster depletion of energy in weakly sheared cases. The first mechanism is unlikely to be important, at least in the subcritical flows; as we show in Sec. IV C, the evolution of the energy for St=4 can be explained in terms of linear processes, whereas wave breaking is a nonlinear process. The second mechanism can be evaluated by examining the budget of turbulent kinetic energy $q^2/2$. For homogeneous turbulence, the turbulent kinetic energy (TKE) equation reads

$$\frac{\partial}{\partial t}\left(\frac{q^2}{2}\right) = P - B - \varepsilon \tag{14}$$

where $P=-\overline{uw}S$ is the production and $B=-g\alpha\overline{wT}$ is the buoyancy flux. In unsheared flow, production is zero, and the

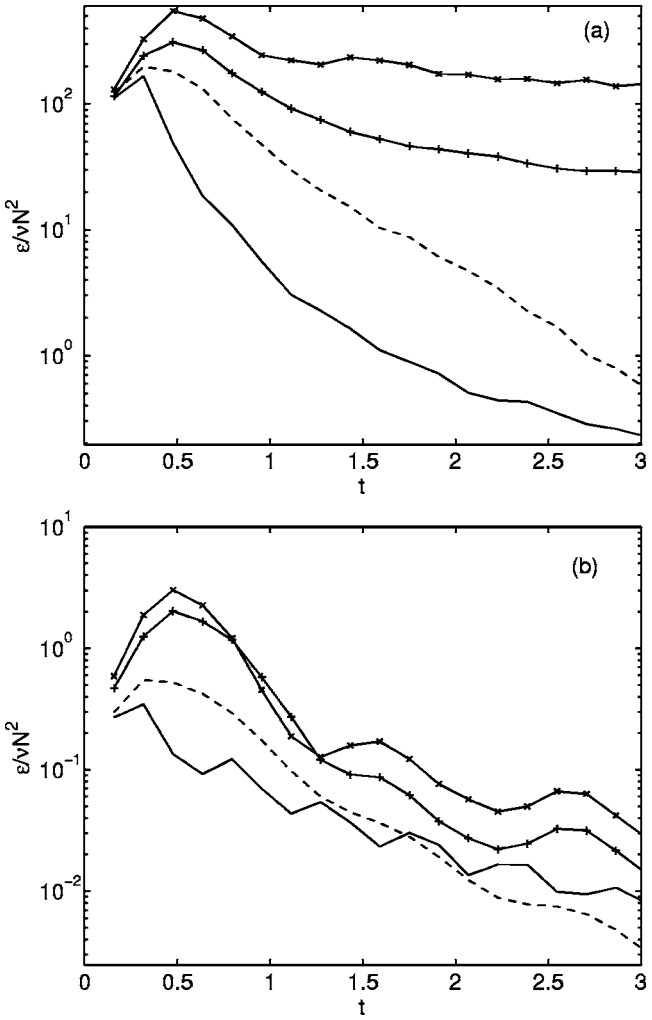

FIG. 7. Normalized rate of dissipation of turbulent kinetic energy: (a) St $=0.25$ and (b) St$=4$. Lines and symbols in (a): unsheared flow (Ri$\rightarrow\infty$) (—); Ri$=1$ (---); 0.25 (+); and 0.16 ($\times$). Lines and symbols in (b): unsheared flow (Ri$\rightarrow\infty$) (—); Ri$=1$ (---); 0.16 (+); and 0.08 ($\times$).

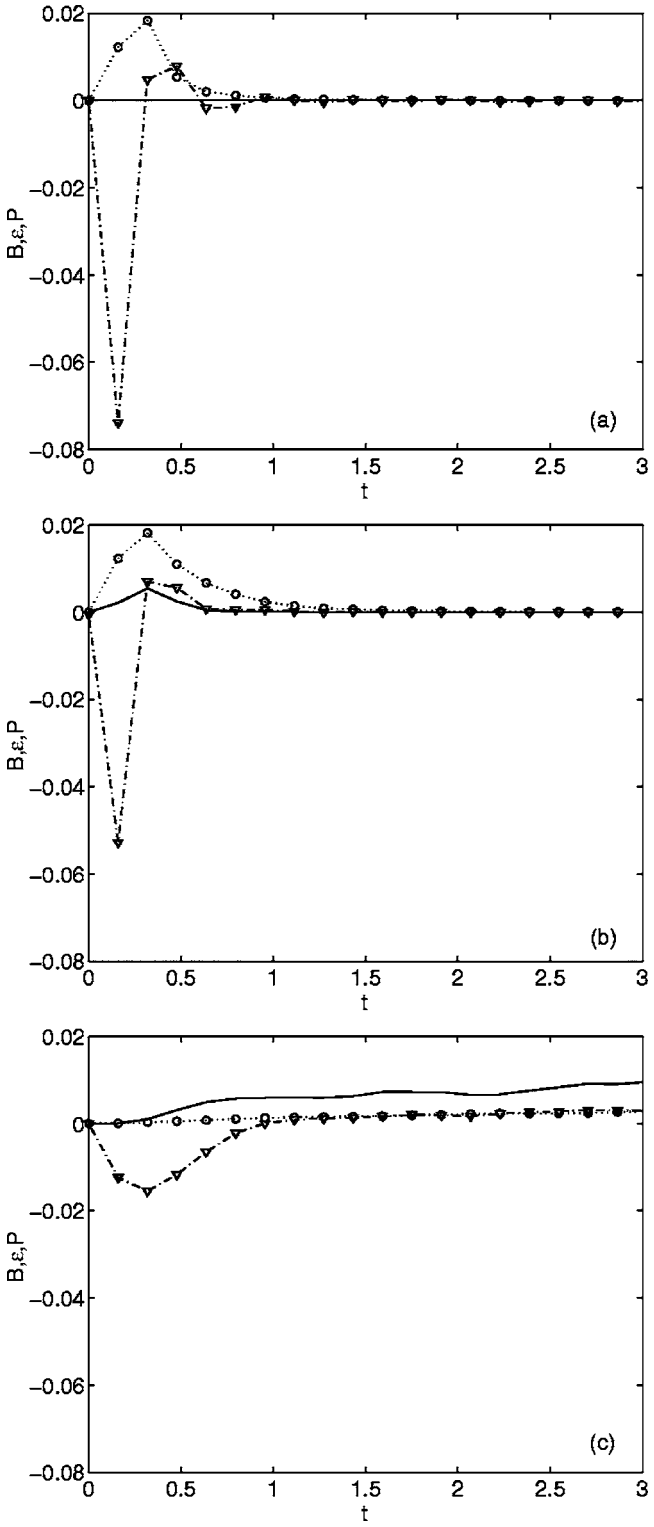

FIG. 8. Energy budgets for (a) unsheared turbulence: St$=0.25$ and Ri$\rightarrow\infty$; (b) weakly sheared turbulence: St$=0.25$ and Ri$=1$; and (c) growing turbulence: St$=0.1$ and Ri$=0.25$. The lines are production (P) (—); buoyancy flux (B) (-▽-); and dissipation (ε) (-○-).

buoyancy flux changes from a source (up-gradient flux, $B<0$) to a sink (down-gradient flux, $B>0$) [Fig. 8(a)]. For Ri$=1$, the production is nonzero until approximately $t=0.6$; although the Reynolds stress becomes up-gradient [Fig. 6(a)], effects of negative production on the TKE are small. Dissipation is larger and the source of TKE from up-gradient buoyancy flux is smaller for Ri>1 than for the unsheared flow. The case with growing turbulence has sustained production and dissipation and active mixing for $t>1$ [Fig. 8(c)]. As Ri decreases, the source of TKE from up-gradient buoyancy flux decreases. Therefore, growing turbulence is due to sustained production, whereas the greater energy depletion in weakly sheared cases is due mainly to shear reducing the up-gradient flux and partially to increased dissipation.

C. Comparison with RDT

If the argument regarding St in Sec. II B holds, RDT should predict the flow evolution for large St. This argument is supported by the estimates of Rehmann and Hwang[20] and the low values of $\varepsilon/\nu N^2$ for subcritical flows [Fig. 7(b)]. In fact, RDT reproduces many features of the evolution of the rms quantities for St$=4$ (Fig. 9). RDT predicts the qualitative trend in both u and w, and it captures the difference in oscillation frequency between the two components. Like DNS, RDT shows that u decreases with increasing Richardson

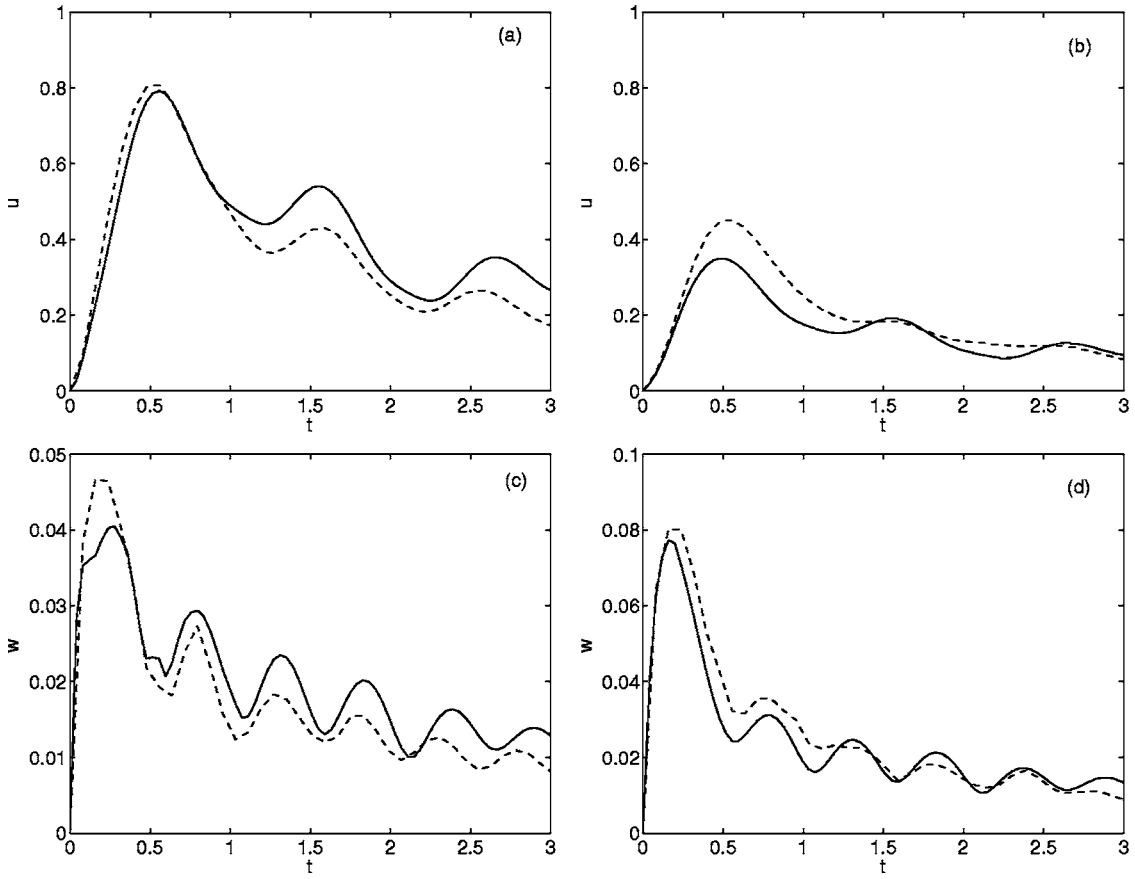

FIG. 9. Comparison of RDT and DNS for St=4: (a) rms streamwise velocity fluctuation for Ri=0.01, (b) rms streamwise velocity fluctuation for Ri=0.08, (c) rms vertical velocity fluctuation for Ri=0.01, and (d) rms vertical velocity fluctuations for Ri=0.08. Dotted lines indicate results from RDT and solid lines are the results of DNS. Vertical scales in (c) and (d) differ.

number, whereas w increases with increasing Richardson number. Quantitative differences between RDT and DNS occur at this finite value of St: At later times RDT underpredicts the rms quantities for Ri=0.01 and overpredicts u for Ri=0.08. Early in the evolution, when the initial temperature fluctuations are adjusting under gravity, the linear theory overpredicts both velocity components.

RDT also reproduces the observation from DNS that energy in weakly sheared flows is smaller than that in unsheared flow. Although RDT overpredicts the total energy slightly, the theoretical results (Fig. 10) match the DNS results [Fig. 3(b)] quite well. For all Ri, RDT captures the decrease in energy, the oscillations, and their frequency, and it accurately estimates the time at which the total energy of the flow with Ri=1 falls below that of the unsheared flow. The success of RDT in predicting the energy evolution suggests that the decrease of energy in weakly sheared flows is due to linear, rather than nonlinear, processes.

V. SUMMARY

We investigated the dynamics of turbulence activated by remnant potential energy in a sheared, stratified flow. At small times, production of kinetic energy by shear is unimportant, and the flow evolves as in the unsheared case. Later in the evolution, effects of the stratification number St and the gradient Richardson number Ri become more important. In particular, flow properties depend on whether the flow is supercritical (St$<$1) or subcritical (St$>$1). Only supercritical flows have active mixing, as indicated by the normalized dissipation. Also, although the rms streamwise velocity increases with increasing shear in all cases, the rms tempera-

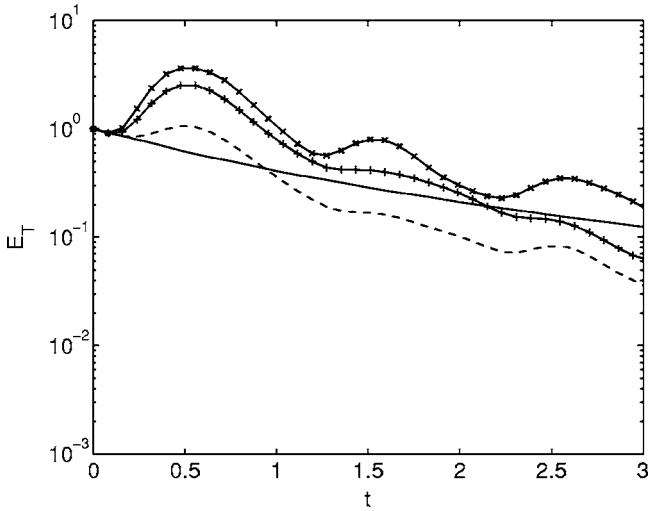

FIG. 10. RDT predictions of total energy for St=4: unsheared flow (Ri $\rightarrow\infty$) (—); Ri=1 (---); 0.16 (-+-); and 0.08 (-×-). This plot can be compared with the DNS results in Fig. 3(b).

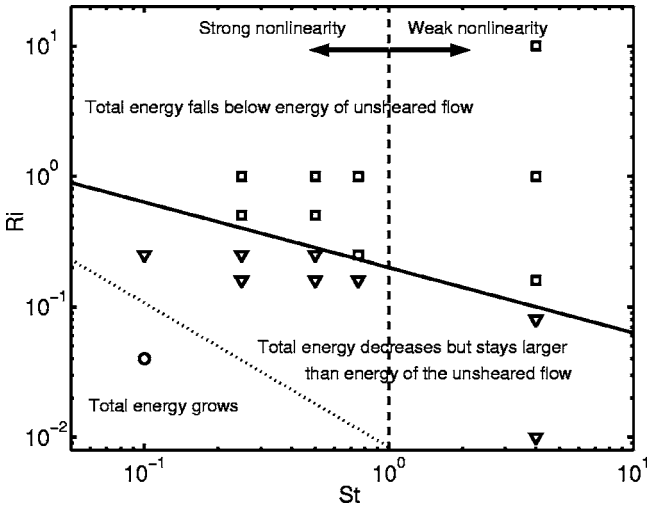

FIG. 11. Summary of flow states. The circle indicates a flow with increasing total energy. The triangles indicate flows with total energy that decreases but remains greater than that of the unsheared case with the same St. The squares indicate flows with total energy decreasing below that of the unsheared case with the same St. Lines are sketched qualitatively to separate the flow states.

ture and vertical velocity increase with increasing shear in supercritical flows but decrease with increasing shear in subcritical flows. The energy of the flow decreases in time in all cases except for one with low values of both St and Ri. Although energy in strongly sheared flows exceeds that in the unsheared flow with the same St, when shear is weak, the total energy decreases below that of the unsheared case. The flow states are summarized as a function of Richardson number and stratification number in Fig. 11.

The simulations provide further information on the energy depletion in weakly sheared flows. Although Reynolds stress can be up-gradient, effects of negative production are small. Compared to the unsheared case, shear increases the dissipation and reduces the source of turbulent kinetic energy from up-gradient buoyancy flux. Time scale arguments involving St and small values of $\varepsilon/\nu N^2$ suggest that subcritical flow is almost linear, and rapid distortion theory reproduces many features of the evolution of rms quantities and the energy. In particular, RDT results suggest that the energy depletion in weakly sheared flows is due mainly to linear processes.

ACKNOWLEDGMENTS

Two of the authors (J.H.H. and C.R.R.) acknowledge support from the National Science Foundation under Grant No. 01-17782. Another author (H.Y.) was supported by a Grant-in-Aid for Science Research (B2) 16310005 from the Japan Society for the Promotion of Science.

[1] T. Gerz, U. Schumann, and S. E. Elghobashi, "Direct numerical simulation of stratified homogeneous turbulent shear flows," J. Fluid Mech. **200**, 563 (1989).
[2] D. Ramsden and G. Holloway, "Energy transfers across an internal wave-vortical mode spectrum," J. Geophys. Res. **97**, 3659 (1992).
[3] J. Woods, V. Hogstrom, P. Misme, H. Ottersten, and O. M. Phillips, "Fossil turbulence," Radio Sci. **4**, 1365 (1969).
[4] P. W. Nasmyth, "Ocean turbulence," Ph.D. thesis, University of British Columbia (1970).
[5] C. H. Gibson, V. Nabatov, and R. Ozmidov, "Measurement of turbulence and fossil turbulence near Ampere seamount," Dyn. Atmos. Oceans **19**, 175 (1993).
[6] T. Gerz and U. Schumann, "Direct simulation of homogeneous turbulence and gravity waves in sheared and unsheared stratified flows," in *Turbulent Shear Flows 7*, edited by F. Durst *et al.* (Springer, New York, 1991), p. 27.
[7] J. J. Rohr, E. C. Itsweire, K. N. Helland, and C. W. Van Atta, "Growth and decay of turbulence in a stratified shear flow," J. Fluid Mech. **195**, 77 (1988).
[8] S. E. Holt, J. R. Koseff, and J. H. Ferziger, "A numerical study of the evolution and structure of homogeneous stably stratified sheared turbulence," J. Fluid Mech. **237**, 499 (1992).
[9] F. G. Jacobitz, S. Sarkar, and C. W. Van Atta, "Direct numerical simulations of the turbulence evolution in a uniformly sheared and stably stratified flow," J. Fluid Mech. **342**, 231 (1997).
[10] L. H. Shih, J. R. Koseff, J. H. Ferziger, and C. R. Rehmann, "Scaling and parameterization of stratified homogeneous turbulent shear flow," J. Fluid Mech. **412**, 1 (2000).
[11] T. Gerz and H. Yamazaki, "Direct numerical simulation of buoyancy driven turbulence in stably stratified fluid," J. Fluid Mech. **249**, 415 (1993).
[12] T. Gerz and H. Yamazaki, "Buoyancy driven turbulence in shear flow," Ninth Symposium on Turbulence Shear Flows, Kyoto, Japan (1993).
[13] H. Hanazaki and J. C. R. Hunt, "Linear processes in unsteady stably stratified turbulence," J. Fluid Mech. **318**, 303 (1996).
[14] J. T. Lin and Y. H. Pao, "Wakes in stratified fluids," Annu. Rev. Fluid Mech. **11**, 317 (1979).
[15] J. H. Lienhard V and C. W. Van Atta, "The decay of turbulence in thermally stratified flow," J. Fluid Mech. **210**, 57 (1990).
[16] W. D. Smyth and J. N. Moum, "Length scales of turbulence in stably stratified mixing layers," Phys. Fluids **12**, 1327 (2000).
[17] H. Yamazaki, "Stratified turbulence near a critical dissipation rate," J. Phys. Oceanogr. **20**, 1583 (1990).
[18] L. H. Shih, J. R. Koseff, G. N. Ivey, and J. H. Ferziger, "Parameterization of turbulent fluxes and scales using homogeneous sheared stably stratified turbulence simulations," J. Fluid Mech. **525**, 193 (2005).
[19] T. R. Osborn, "Estimates of the local rate of vertical diffusion from dissipation measurements," J. Phys. Oceanogr. **10**, 83 (1980).
[20] C. R. Rehmann and J. H. Hwang, "Small-scale structure of strongly stratified turbulence," J. Phys. Oceanogr. **35**, 151 (2005).